Do Rhodium Bis(σ-amine-borane) Complexes Play a Role as Intermediates in Dehydrocoupling Reactions of Amine-boranes?

DATASET · OCTOBER 2013

READS
41

3 AUTHORS:

Valeria Butera
Technion - Israel Institute of Technology
7 PUBLICATIONS **42** CITATIONS
SEE PROFILE

Nino Russo
Università della Calabria
509 PUBLICATIONS **7,856** CITATIONS
SEE PROFILE

Emilia Sicilia
Università della Calabria
150 PUBLICATIONS **1,919** CITATIONS
SEE PROFILE

CHEMISTRY
A EUROPEAN JOURNAL

DOI: 10.1002/chem.201102365

Do Rhodium Bis(σ-amine-borane) Complexes Play a Role as Intermediates in Dehydrocoupling Reactions of Amine-boranes?

Valeria Butera, Nino Russo, and Emilia Sicilia*[a]

Abstract: The recently synthesized rhodium complex $[Rh\{P(C_5H_9)_2(\eta^2\text{-}C_5H_7)\}(Me_2HNBH_3)_2]BAr^F{}_4$ (**2**), which incorporates two amine-boranes coordinated to the rhodium center with two different binding modes, namely η^1 and η^2, has been used to probe whether bis(σ-amine-borane) motifs are important in determining the general course of amine-boranes dehydrocoupling reactions. DFT calculations have been carried out to explore mechanistic alternatives that ultimately lead to the formation of the amine-borane cyclic dimer $[BH_2NMe_2]_2$ (**A**) by hydrogen elimination. Sequential concerted, on- or off-metal, intramolecular dehydrogenations provide two coordinated amine-borane molecules. Subsequent dimerization is likely to occur off the metal in solution. In spite of the computationally confirmed presence of a BH···NH hydrogen bond between amine-borane ligands, neither a simple intermolecular route for dehydrocoupling of complex **2** is operating, nor seems $[Rh\{P(C_5H_9)_2(\eta^2\text{-}C_5H_7)\}\mathbf{B}]^+$ to be important for the whole dehydrocoupling process.

Keywords: Amine-boranes · catalysis · dehydrocoupling · density functional theory · rhodium

Introduction

The widespread use of hydrogen as an energy carrier to achieve sustainable mobility is of top priority.[1,2] A key obstacle to commercialization of hydrogen-powered, fuel-cell (FC) vehicles is the current lack of a safe and practical method for on-board storage of hydrogen. In this context, storage of hydrogen in a chemical compound through a reversible chemical reaction is a promising strategy.[3,4]

Ammonia borane (NH_3BH_3, AB) and related amine-boranes (R_2HNBH_3) have emerged as attractive candidates for hydrogen-storage materials because of the high availability of hydrogen content[5] and the potential reversibility of the dehydrogenation reactions.[6] Because thermal decomposition of amine-boranes exhibits high kinetic barriers, in the last years, a series of new, and in many cases improved, catalysts for AB and amine-borane adducts dehydrocoupling based on a variety of early and late transition metals have been developed.[7–21] Comprehensive and detailed reviews, which cover the chemistry of AB and related compounds and their potential as hydrogen-storage materials up to early 2010, are available.[22] Despite the number of organometallic complexes that are able to induce the dehydrogenation of amine-borane adducts, the knowledge of the way in which amine-boranes approach, bind, and dehydrocouple at the metal center remains scarce. Such knowledge is crucial for the control of the kinetics of hydrogen release and product distribution. Experimental and computational mechanistic investigations have shown that transition-metal-mediated dehydrocoupling reactions of amine-boranes are very complex processes and both the mechanism and the final outcome depend on the identity of the amine-borane and the metal center.[23]

Two possible general pathways for the first step of the process, that is, dehydrogenation to form an amine-borane ($R_2N=BH_2$), have been proposed. The process might be inner sphere, which involves stepwise or concerted BH/NH transfer pathways at the metal center.[24] All hypothesized dehydrogenation routes involve σ complexes of amine-boranes as reaction intermediates. The process can also be outer sphere, similar to that invoked for transfer dehydrogenation of alcohols, in which a ligand also assists hydrogen transfer.[14,25] Subsequent oligomerization, polymerization, or dimerization of $R_2N{=}BH_2$ can occur either on or off the metal with or without the further involvement of R_2HNBH_3. A further step toward the elucidation of the intricate mechanism of these reactions has been made by Weller and collaborators on rhodium complexes[23c,26] and Alcaraz and Sabo-Etienne on ruthenium complexes.[27] Weller and coworkers have developed systems, which are able to provide key information on the nature of intermediates generated during the dehydrogenation of amine-boranes, from unsaturated cationic rhodium species. The synthesis and solution and solid-state structures of such complexes with a unique bis(σ-amine-borane) bonding mode have been reported recently.[28] These complexes, which give the opportunity to obtain new insights into bonding modes of amine-borane ligands at transition-metal centers, also proceed to dehydro-

[a] V. Butera, Prof. N. Russo, Prof. Dr. E. Sicilia
Department of Chemistry
Università della Calabria
87036 Arcavacata di Rende
Fax: (+39) 0984 492044
E-mail: siciliae@unical.it

Supporting information for this article is available on the WWW under http://dx.doi.org/10.1002/chem.201102365.

genate amine-boranes to form cyclic dimers and trimers and can, therefore, be investigated to gain mechanistic information on the catalytic dehydrogenative coupling of amine-boranes.

Density functional theory (DFT) has been used here to evaluate possible mechanistic routes of the dehydrocoupling reaction of the prototypical, secondary, dimethylamine-borane (Me_2HNBH_3, DMAB) by starting from the bis(σ-amine-borane) complex that is formed by displacement of the labile fluoroarene ligand in the phosphine/alkene complex $[Rh(\eta^6\text{-}C_6H_5F)\{P(C_5H_9)_2(\eta^2\text{-}C_5H_7)\}]BAr^F{}_4$ (**1**) and coordination of two DMAB ligands (see Scheme 1).[27] The formed $[Rh\{P(C_5H_9)_2(\eta^2\text{-}C_5H_7)\}(Me_2HNBH_3)_2]BAr^F{}_4$ complex (**2**) reacts in either mono- or difluorobenzene to yield the cyclic dimer $[BH_2NMe_2]_2$ (**A**) as the main product of dehydrocoupling.

As the aim of the present work is to explore the involvement of complexes with bis(σ-amine-borane) binding motifs as intermediates of amine-boranes dehydrocoupling reactions, only pathways along which coordination of B–N units to the metal center is retained have been examined.

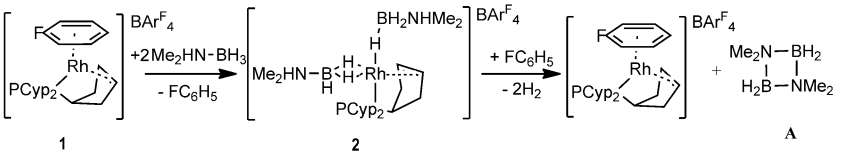

Scheme 1.

Results and Discussion

Complex **2** has been isolated and characterized both in solution and the solid state.[28] The DFT-calculated structure confirms the pseudo-octahedral geometry at the rhodium center and the η^1 and η^2 coordinations of the apical and equatorial amine-borane ligands, respectively. The fully optimized structure of the cationic portion of the 18-electron bis(σ-amine-borane) complex **2** is shown in Figure 1, in which the experimental and theoretical values of the most significant geometrical parameters are compared. Calculated geometrical parameters closely mirror those experimentally observed, with the exception, as expected, of the distance between the H1c and H2 hydrogen atoms of the amine-borane ligands. Calculations allow a more secure location of the hydrogen atoms involved in the BH···HN hydrogen-bonding interaction with respect to the values extracted from the crystallographic characterization of the complex. The Supporting Information gives atomic coordinates for the complex.

Scheme 2 provides an overview of the possible reaction routes that can be proposed on the basis of experimental findings and our computational results for the subsequent

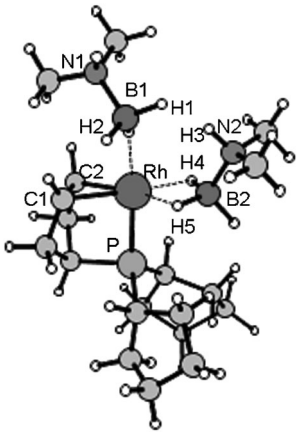

Figure 1. DFT-optimized geometrical structure of cationic part of **2**. Selected bond lengths (Å) compared with available experimental values (in parentheses): Rh–B1 = 2.696 (2.661), Rh–B2 = 2.288 (2.282), Rh–P = 2.257 (2.2197), Rh–C1 = 2.108 (2.106), Rh–C2 = 2.119 (2.121), C1–C2 = 1.432 (1.417), H1–H3 = 1.686 (*2.12*).

dehydrogenation of the two amine-borane ligands of complex **2** to afford the cyclic dimer **A** alongside H_2 release.

Even though the 18-electron complex **1** is the organometallic precatalyst in fluorobenzene solvent, the mechanistic investigation really starts from complex **2**, because the first step in any mechanism is likely to be dissociation of the bound arene solvent in **1**. The study only takes into consideration the energetics for the formation of **2** by dissociation of the solvent molecule and coordination of two DMAB molecules (see Figure 2). The process is calculated to be exergonic by 13.5 and 9.3 kcal mol^{-1} in gas phase and solution, respectively.

To discuss the reaction mechanism of dehydrocoupling, it is necessary to consider two possible alternative pathways, that is, inter- and intramolecular dehydrogenations. On the basis of a syntax already introduced in the former mechanism,[20] one of the hydridic BH atoms of the apical DMAB molecule interacts with the acidic NH proton of the other molecule in equatorial position to release H_2 and form a B–N bond. Due to the presence of the BH···HN hydrogen bond, Weller and co-workers have suggested that a dehydrocoupling pathway, which proceeds in an intermolecular fashion by simple H_2 loss, might be low-energy.[28] The formed linear dimer $Me_2HNBH_2NMe_2BH_3$ (**B**) could undergo further dehydrocoupling directly on the metal center to give **A**. The pathway labeled (c) corresponds to such a hypothesis, whereas in the intramolecular dehydrogenation processes, labeled (a) and (b), BH and NH hydrogen atoms are eliminated from the same molecule to give the bound monomer $Me_2N{=}BH_2$ and molecular hydrogen. BH/NH activation occurs by (stepwise or concerted) hydrogen transfer to the metal along pathway (a) and off-metal dehydrogenation by

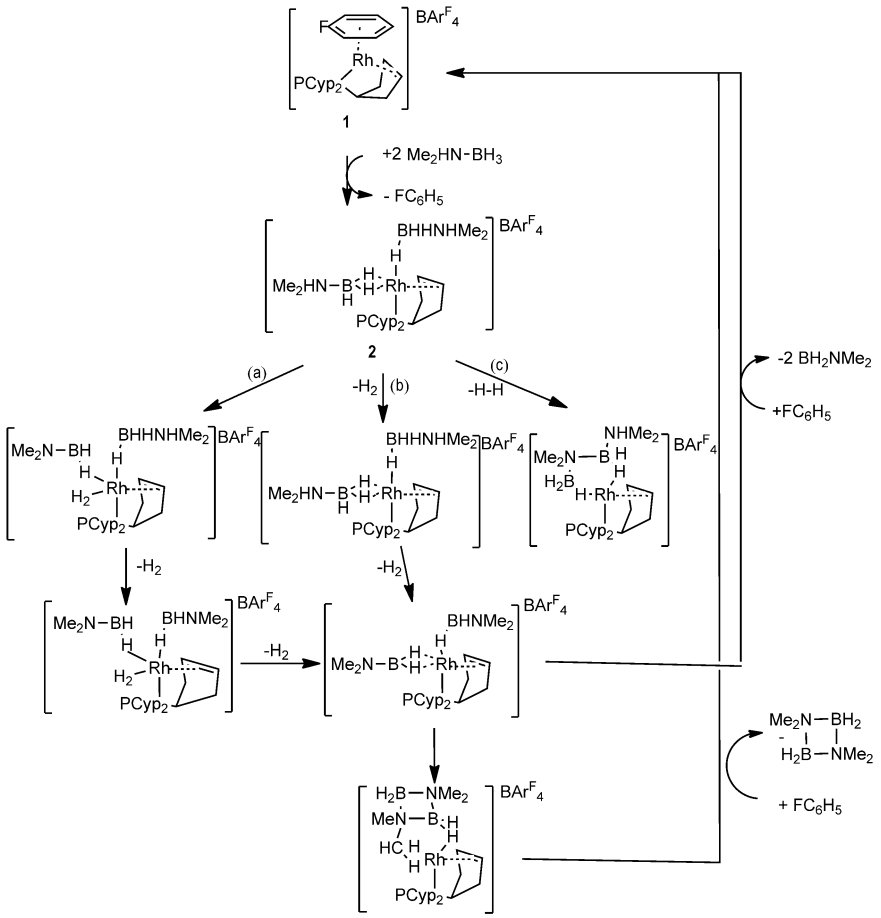

Scheme 2. Overview of alternative dehydrocoupling pathways.

simultaneous B–H and N–H bonds cleavage along pathway (b), respectively. Formed $Me_2N{=}BH_2$ monomers then undergo further reactivity on or off the metal to afford **A**. Along all the examined pathways pseudo-octahedral coordination and 18-electron count at the metal center are conserved. Calculated energy profiles are reported in Figure 2–4, except for pathway (c), for reasons that will become clear soon, and will be illustrated in the next paragraphs. Unless otherwise noted, the discussed energies are free energies in solution (ΔG) calculated with respect to asymptote of the reactant: **1**+2DMAB. Optimized geometrical structures of stationary points are also sketched in Figure 2–4, whereas the Supporting Information gives the calculated values for the most relevant geometrical parameters and Cartesian coordinates for all the structures reported herein. All geometry optimizations have been performed by including an explicit fluoroarene solvent molecule.

Intramolecular on-metal dehydrogenation: The outcomes of the investigation of the intramolecular, dehydrogenation pathway (a) are shown in Figure 2.

Although calculations have been carried out to locate stationary points for both concerted and stepwise BH/NH activations, all attempts to model a stepwise mechanism by location of minima and transition state corresponding to the BH transfer to the Rh center followed by NH activation have failed. Once the bis(σ-amine-borane) complex is formed by displacement of the fluoroarene ligand, the dehydrogenation proceeds by concerted hydrogen transfer from the equatorial DMAB molecule to the metal center through transition state $\mathbf{TS_{2\text{-}3}}$, with a very high free-energy barrier of 48.3 kcal mol^{-1} to afford the Rh–dihydrogen intermediate **3**. In $\mathbf{TS_{2\text{-}3}}$, the NH proton is drawn toward the metal center, and the coordinated BH bond is significantly stretched (B···H(Rh) = 3.001 Å). The produced metal-bound $Me_2N{=}BH_2$ molecule is η^1 coordinated in intermediate **3** with a hydrogen molecule as the fourth ligand in the equatorial plane. Intermediate **3** is less stable than **2** by 10.2 kcal mol^{-1}. H_2 loss from **3** occurs by η^2 coordination of $Me_2N{=}BH_2$ with a low energy barrier of 2.6 kcal mol^{-1} ($\mathbf{TS_{3\text{-}4}}$). From the formed intermediate **4**, which lies 2.3 kcal mol^{-1} below complex **3**, the dehydrocoupling reaction proceeds by Rh-mediated dehydrogenation of the axial DMAB molecule through $\mathbf{TS_{4\text{-}5}}$

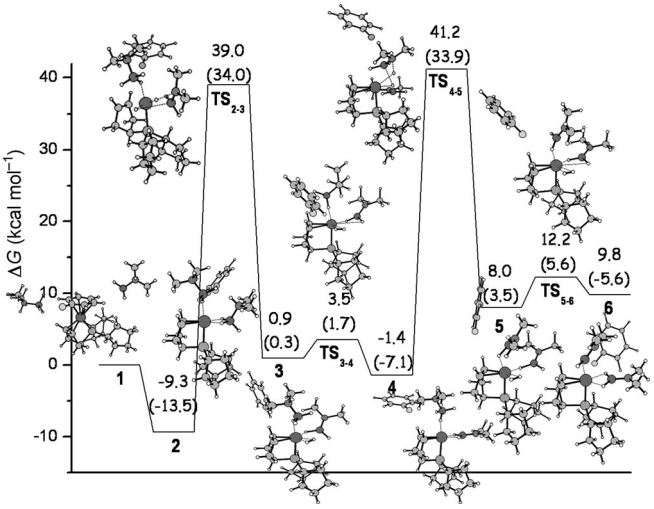

Figure 2. Calculated B3PW91 free-energy profile for the sequential, intramolecular (pathway (a)), metal-assisted, dehydrogenation reaction of amine-borane ligands in the bis(σ-amine-borane) complex **2**. Gas-phase, zero-point-corrected energy changes are reported in parentheses. Energies are in kcal mol^{-1} and relative to the asymptote of the reactant.

with a free-energy barrier of 42.6 kcal mol^{-1}. Similar to $\mathbf{TS_{2\text{-}3}}$, the NH proton approaches the Rh center, whereas the BH hydride is almost detached (B···H(Rh) = 2.359 Å). The high energy barriers associated with the dehydrogenation reactions are reflected by the slow rates and the high catalytic loadings experimentally detected.[28] From intermediate **5**, for which the formation is endergonic by 9.4 kcal mol^{-1} with respect to **4**, a second hydrogen molecule is released to yield the final product (**6**) of the dehydrogenation reaction of both equatorial and axial DMAB molecules. Also in this case, the first-formed, amine-borane, equatorial molecule assists the H_2 release by changing the coordination mode from η^1 to η^2 with a barrier of 4.2 kcal mol^{-1}. The ability to switch from η^2 to η^1 coordination mode and vice versa is a very attractive feature of boron-hydride-containing ligands.[29] Formation of **6** is calculated to be endergonic with respect to the reactants by 9.8 kcal mol^{-1}.

The mechanism proposed here differs from that put forward for $[Rh(P\mathit{i}Bu_3)_2]^+$, for which pathways that involve sequential N–H/B–H or B–H/N–H activation have been found to be competitive,[23c] and the N–H activation to be the rate-limiting step.

Coupling of amine-boranes: Figure 3 shows the energy profiles for the second part of the dehydrocoupling process. That is, once **6** is formed, the metal-bound $Me_2N{=}BH_2$ monomers further react to give the cyclic dimer **A**. The coupling reaction can occur either directly on the metal center by formation of two new B–N covalent bonds between the two amine-borane ligands that approach each other or off the metal by release of the two $Me_2N{=}BH_2$ molecules that then can dimerize in solution to provide **A**. The cyclic dimer **A** formed in the former case is released by coordination to two DMAB ligands or to a solvent molecule. Because Weller and co-workers have underlined that in fluorobenzene solvent together with **A** the final organometallic product is **1**,[28] we have computed the energetic cost for the displacement of both the cyclic dimer and amine-borane due to coordination to the fluoroarene ligand to regenerate precatalyst **1**. Minima and transition states along both these two alternative pathways have been intercepted and energetics and structures are reported in Figure 3.

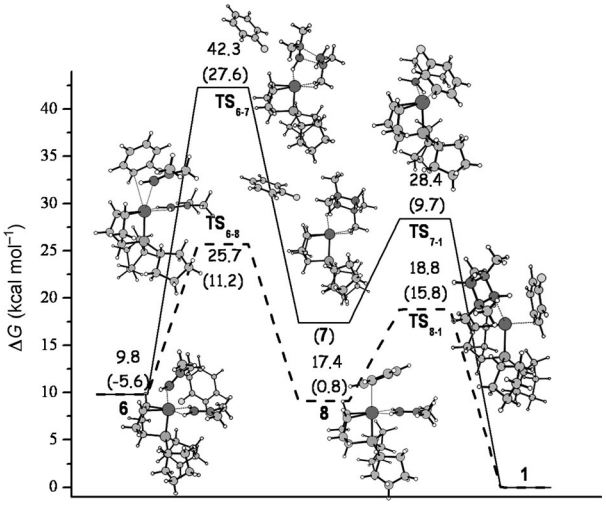

Figure 3. Calculated B3PW91 free-energy profiles for the on-metal coupling reaction of metal-bound amine-borane ligands and subsequent release of cyclic dimer **A** and alternative solvent-induced, sequential, amine-borane-ligands release. Gas-phase, zero-point-corrected energy changes are reported in parentheses. Energies are in kcal mol^{-1} and relative to the **1**+2DMAB asymptote of the reactants.

Direct coupling of two $Me_2N{=}BH_2$ amine-borane monomers on the metal center to afford the cyclic $[BH_2NMe_2]_2$ occurs by surmounting a free-energy barrier of 32.5 kcal mol^{-1}, which corresponds to $\mathbf{TS_{6\text{-}7}}$. The normal mode associated with the imaginary frequency, calculated to be 382i cm^{-1}, corresponds to the stretching of the N–B intramolecular double bonds and incipient formation of new intermolecular N–B bonds. The axial amine-borane ligand maintains the BH η^1 coordination with the metal center. The equatorial $Me_2N{=}BH_2$ monomer has to rotate, release the BH η^2 coordination, and recoordinate to the metal center through a CH_3 group to be properly oriented with respect to the axial monomer (see Figure 3). Unfortunately, intrinsic reaction coordinate (IRC) calculations are not able to clearly identify the minimum connected to the transition state on the reactant side. We can only guess that the required rearrangement is not straightforwardly accomplished. As a result, $[BH_2NMe_2]_2$ rhodium complex **7**, which is less stable than intermediate **6** by 7.6 kcal mol^{-1}, is formed. Calculations reveal a pseudo-octahedral Rh center coordinated in a η^2/η^1 mode with the $[BH_2NMe_2]_2$ ligand (see Figure 3 and the Supporting Information). A B–H bond in axial position establishes η^1 coordination, whereas η^2 coordination is due to one of the CH_3 groups in equatorial position. The $[BH_2NMe_2]_2$ product is released and catalyst **1** restored by coordination of a solvent molecule through $\mathbf{TS_{7\text{-}1}}$ with a barrier of 11.0 kcal mol^{-1} in fluorobenzene. To first displace the axial ($\mathbf{TS_{6\text{-}8}}$) and subsequently the equatorial ($\mathbf{TS_{8\text{-}1}}$) $Me_2N{=}BH_2$ monomers, it is necessary to overcome individual free-energy barriers that are estimated to be 15.9 and 9.7 kcal mol^{-1}, respectively. Because of the unfavorable energetics of the formation of the cyclic dimer directly on the metal center, our computational analysis suggests dimerization off the metal to be operative for the formation of product **A**. At the same level of theory (see the Supporting Information), uncatalyzed dimerization is exergonic, as expected,[23d] and the calculated free-energy barrier of 20.5 kcal mol^{-1}, which is in good agreement with that determined experimentally,[30] confirms that free monomers should dimerize in solution.

Intramolecular off-metal dehydrogenation: The intramolecular elimination of molecular hydrogen from each DMAB molecule to provide two-coordinated amine-borane molecules that further dimerize should occur through the alternative pathway (b). The calculated energy profile is shown in Figure 4.

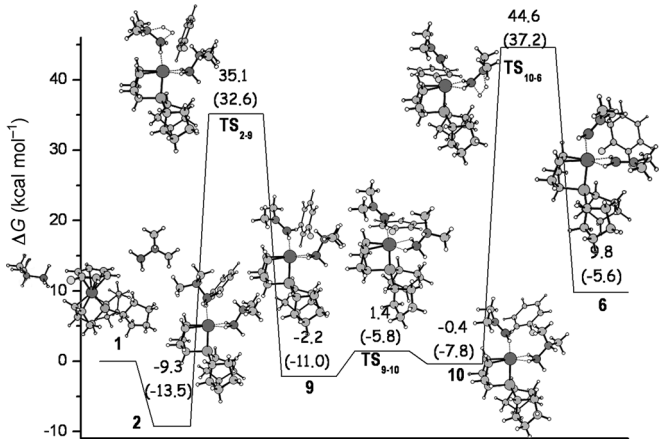

Figure 4. Calculated B3PW91 free-energy profile for the sequential, off-metal, intramolecular, dehydrogenation reaction (pathway (b)) of axial/equatorial amine-borane ligands in the bis(σ-amine-borane) complex **2**. Gas-phase, zero-point-corrected energy changes are reported in parentheses. Energies are in kcal mol^{-1} and relative to the asymptote of the reactants.

Metal coordination, by induction of a charge polarization of the BH hydride, enhances the acidity of the NH proton and, therefore, might facilitate an initial electrostatic interaction between the NH proton and the BH hydride of the same molecule, which should react to eliminate H_2 without the direct involvement of the metal center. The energy profile for the sequential H_2 loss from the axial/equatorial amine-borane molecules is reported in Figure 4. From **2**, formation of the metal-bound amino complex **9** by elimination of molecular hydrogen from the axial DMAB molecule occurs through $\mathbf{TS_{2\text{-}9}}$ with a free-energy barrier of 44.4 kcal mol^{-1}. Complex **9** lies 2.2 kcal mol^{-1} below the energy of the separate reactants. For the elimination of H_2 from the equatorial amine-borane ligand to occur, the NH proton needs to point in the same direction as the BH hydride that is not involved in the coordination to the metal center. Such a geometry is realized in an isomer of **9**, which can be obtained by a rotation around the N–B bond through $\mathbf{TS_{9\text{-}10}}$ with an energy barrier of 3.6 kcal mol^{-1}. Isomer **10**, which is less stable than **9** by 3.2 kcal mol^{-1}, eliminates molecular hydrogen by surmounting a high energy barrier of 45.0 kcal mol^{-1} both in gas phase and in solution. The diamine-borane complex **6** could be analogously formed by sequential H_2 loss from the equatorial/axial amine-borane molecules. Computations show that the energetics is almost unchanged (the energy profile is reported in the Supporting Information). Coupling of amine-borane ligands can proceed to afford the cyclic dimer **A** along the pathways described in Figure 3.

Intermolecular dehydrogenation: Barriers that hamper formation of **6** are very high along both (a) and (b) pathways, even higher than those calculated by us (see Scheme 3) and previously reported for the uncatalyzed dehydrogenation.[20] Nonetheless, on the basis of our computational analysis, dehydrocoupling that occurs by sequential, concerted, intramolecular dehydrogenation of DMAB ligands, irrespective of the mechanism, represents the only viable reaction route to $[BH_2NMe_2]_2$ production. The intermolecular dehydrogenation process should proceed, as pointed out above, by the interaction of the BH hydride of the axial ligand and the NH proton of the equatorial DMAB molecule to release molecular hydrogen and form a B–N bond to afford $Me_2HNBH_2NMe_2BH_3$ directly on the metal center. In spite of the favorable orientation of the BH1c and NH2 hydrogen atoms implicated in a nonclassical hydrogen bond in **2**, all the attempts to computationally model such a pathway have been unsuccessful. The only intercepted transition state, for which the structure seems to correspond to a rearrangement that could be a prelude to the intermolecular dehydrogenation that yields the $[Rh\{P(C_5H_9)_2(\eta^2\text{-}C_5H_7)\}\mathbf{B}]^+$ complex (**11**), is drawn in Figure 5 along the reaction pathway ob-

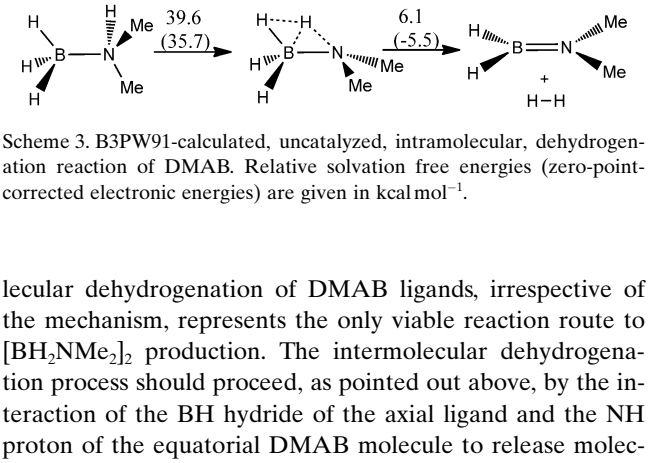

Scheme 3. B3PW91-calculated, uncatalyzed, intramolecular, dehydrogenation reaction of DMAB. Relative solvation free energies (zero-point-corrected electronic energies) are given in kcal mol^{-1}.

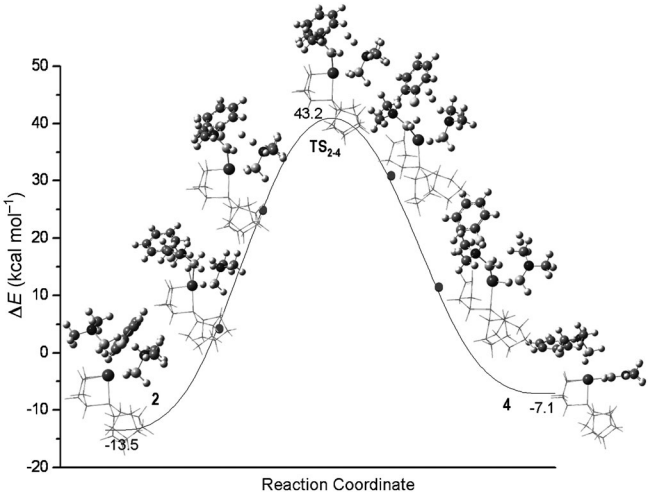

Figure 5. Gas-phase intrinsic reaction-coordinate results from $\mathbf{TS_{2\text{-}4}}$ to **2** and **4** minima. Energies are in kcal mol^{-1}.

tained by IRC calculations. The identified transition state, $\mathbf{TS_{2\text{-}4}}$, is characterized by an imaginary frequency of 466i cm^{-1} and the associated normal mode mainly corresponds to the stretching of the B–H and N–H bonds that release molecular hydrogen.

However, the analysis of the structures along the reaction coordinate from the transition state to the product reveals that H_2 loss is accompanied by the shift of a BH hydride from the boron atom of the equatorial DMAB ligand to the boron atom of the ligand in apical position. In such a rearrangement the hydride is transferred first to the Rh atom, as

it appears in Figure 5, and from the metal to the boron atom of the axial ligand, to form the intermediate complex that we have indicated as **4** in one step along pathway (a). That is, the path sketched in Figure 5 represents an alternative, not competitive, because of the high energy barrier, route for the dehydrogenation of the equatorial DMAB ligand. Moreover, these calculations confirm that monohydride rhodium complexes are not stable intermediates along the pathways considered in the present case. The DFT fully optimized structure of the cationic part of **11**, instead, is shown in Figure 6, in which available experimental geometrical parameters are compared with calculated ones.

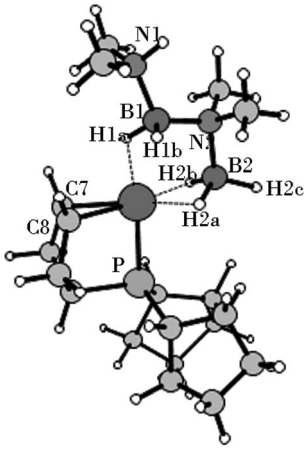

Figure 6. DFT-optimized geometrical structure of cationic portion of **11**. Selected bond lengths (Å) and angles (°) compared with available experimental values (in parentheses): Rh−B1 = 2.594 (2.626), Rh−B2 = 2.247 (2.242), Rh−P = 2.241 (2.2058), Rh−C7 = 2.117 (2.121), Rh−C8 = 2.115 (2.107), Rh−H1a = 1.842 (1.96), Rh−H2a = 1.931 (1.85), Rh−H2b = 1.905 (1.84), C7−C8 = 1.432 (1.417), B1−H1a = 1.258 (1.13), B1−H1b = 1.197 (1.12), B2−H2a = 1.264 (1.23), B2−H2b = 1.268 (1.22), B2−H2c = 1.203 (1.13), B1-N1-B2 = 102.6 (103.3), N1-B1-N2 = 112.7 (112.7), Rh-H1a-B1 = 112.2 (113).

Such a formation of **11** from **2** by intermolecular H_2 elimination and formation of a B−N bond has not been observed.[28] Instead, **11** has been produced by addition of **B** to **1** and displacement of the fluoroarene ligand and characterized both in solution and in the solid state.[31] The η^2/η^1 Rh−B coordination mode of the diborazane ligand is properly reproduced and the computed geometry is in good agreement with the experimental structure.

On the basis of the experimental findings we have excluded that the borazane complex **11** could ultimately afford **A** by intramolecular dehydrocoupling and have suggested that a more complex mechanism should be operative. Additionally, despite repeated attempts, we have not been able to intercept any transition state or identify any pathway that from **2** leads to **11**. Therefore, for **11** to be a viable intermediate in the overall dehydrocoupling process of **2**, a different formation process should be envisaged; this possibly involves further addition of DMAB or **B**.

Conclusion

In an effort to understand the mechanistic scenario for amine-borane dehydrogenation in more detail, we have shown that dehydrocoupling of two DMAB ligands coordinated to the rhodium center with two different bonding modes, namely η^1 and η^2, proceeds by sequential, concerted, intramolecular dehydrogenation, on- or off-metal, to provide two coordinated amine-borane molecules. Energy barriers calculated along the on- and off-metal dehydrogenation pathways are comparable and higher than the estimated barrier for the uncatalyzed DMAB dehydrogenation; this suggests that metal mediation is not beneficial in the present case. Notably, subsequent dimerization is likely to occur off the metal in solution. Although the energetics of sequential, concerted, intramolecular dehydrogenation of DMAB ligands is calculated to be unfavorable, the possibility that H_2 loss occurs by stepwise BH/NH activation can be ruled out because all the strategies used to locate stationary points, which correspond to the formation of monohydride complexes, have failed. In spite of the computationally confirmed presence of a BH···NH hydrogen bond between DMAB ligands, the outcomes of our computations suggest that neither a simple intermolecular route for dehydrocoupling of **2**, nor intermediate **11** seem to play any roles in the whole dehydrocoupling process. Calculations show that the examined rhodium bis(σ-amine-borane) complex sits in a relatively deep energy well and coordination of the amine-borane products that result from dehydrogenation should be achieved, but has a very high energetic cost. Therefore, although complexes with bis(σ-amine-borane) binding modes can be formed during the whole dehydrogenative coupling process, they are not relevant for catalysis. Reported results are of particular interest as they contribute to shed light on the elementary steps of the, not yet established, mechanism of metal-catalyzed amine-boranes dehydrogenation/dehydrocoupling. Future work will address the influence that the identity of the metal and the spectator-ligand environment has on the course of this important transformation.

Computational Details

Geometry optimizations as well as frequency calculations for all reactants, intermediates, products, and transition states were performed at the density functional level of theory by using the B3PW91 functional[32] as implemented by the GAUSSIAN 03[33] code. For Rh the relativistic compact Stuttgart/Dresden effective core potential[34] was used in conjunction with the split valence basis set. The standard 6-311G* basis sets of Pople and co-workers were employed for the rest of the atoms, except C and H atoms of C_3H_9 rings on which the smaller 3-21G basis were used. For each optimized stationary point, vibrational analysis was performed to determine the character (minimum or saddle point) and zero-point vibrational energy (ZPVE) corrections were included in all relative energies (ΔE). For transition states, it was carefully checked that the vibrational mode associated with the imaginary frequency corresponds to the correct movement of involved atoms. Furthermore, the IRC[35] method was used to asses that the localized TSs correctly connect to the corresponding minima along the imaginary mode of vibration. The free energies, G, were calculated for $T = 298.15$ K. All relative energies are reported in

kcal mol^{-1}. Implicit solvent effects were calculated through the integral equation formalism polarizable continuum model (IEFPCM).[36] Because preliminary calculations have clearly shown that geometry relaxation effects are not significant, single-point calculations were performed by using more extended 6-311+G** basis sets, except for Rh on fully optimized geometry of each stationary point along the reaction paths. Calculations were carried out in dichloroethane ($\varepsilon = 10.36$) as a mimic of fluoroarene solvent. Reaction Gibbs free energies in solution (ΔG_{sol}) were calculated for each process as the sum of two contributions: a gas-phase-reaction free energy (ΔG_{gas}) and a solvation-reaction free-energy term calculated with the continuum approach (ΔG_{solv}).

Acknowledgements

This research was supported by Università della Calabria and was carried out within the FP7 project HYPOMAP (project no. 233482).

[1] R. Coontz, B. Hanson, *Science* **2004**, *305*, 957.
[2] G. W. Crabtree, M. S. Dresselhaus, M. V. Buchanan, *Phys. Today* **2004**, *57*, 39.
[3] U. S. DOE. Hydrogen, Fuel Cells & Infrastructure Technology Program (http://www.eere.energy.gov/hydrogenandfuelcells/storage).
[4] The American Physical Society. The Hydrogen Initiative (http://www.aps.org/public_affairs/index.cfm).
[5] U. S. DOE. Basic Research Needs for the Hydrogen Economy (http://www.sc.doe.gov/bes/reports/files/NHE_rpt.pdf).
[6] a) D. A. Dixon, M. Gutowski, *J. Phys. Chem. A* **2005**, *109*, 5129; b) A. Staubitz, M. Besora, J. N. Harvey, I. Manners, *Inorg. Chem.* **2008**, *47*, 5910–5918.
[7] M. Zahmakiran, S. Özkar, *Inorg. Chem.* **2009**, *48*, 8955–8964.
[8] M. E. Sloan, T. J. Clark, I. Manners, *Inorg. Chem.* **2009**, *48*, 2429–2435.
[9] C. Y. Tang, A. L. Thompson, S. Aldridge, *Angew. Chem.* **2010**, *122*, 933–937; *Angew. Chem. Int. Ed.* **2010**, *49*, 921–925.
[10] R. Rousseau, G. K. Schenter, J. L. Fulton, J. C. Linehan, M. H. Engelhard, T. Autrey, *J. Am. Chem. Soc.* **2009**, *131*, 10516–10524.
[11] Y. Jiang, O. Blacque, T. Fox, C. M. Frech, H. Berke, *Organometallics* **2009**, *28*, 5493–5504.
[12] A. Staubitz, A. P. Soto, I. Manners, *Angew. Chem.* **2008**, *120*, 6308–6311; *Angew. Chem. Int. Ed.* **2008**, *47*, 6212–6215.
[13] T. M. Douglas, A. B. Chaplin, A. S. Weller, *J. Am. Chem. Soc.* **2008**, *130*, 14432–14433.
[14] N. Blaquiere, S. Diallo-Garcia, S. I. Gorelsky, D. A. Black, K. Fagnou, *J. Am. Chem. Soc.* **2008**, *130*, 14034–14034.
[15] D. Pun, E. Lobkovsky, P. J. Chirik, *Chem. Commun.* **2007**, 3297–3299.
[16] Y. Jiang, H. Berke, *Chem. Commun.* **2007**, 3571–3573.
[17] J. L. Fulton, J. C. Linehan, T. Autrey, M. Balasubramanian, Y. Chen, N. K. Szymczak, *J. Am. Chem. Soc.* **2007**, *129*, 11936–11949.
[18] M. C. Denney, V. Pons, T. J. Hebden, D. M. Heinekey, K. I. Goldberg, *J. Am. Chem. Soc.* **2006**, *128*, 12048–12049.
[19] a) C. A. Jaska, K. Temple, A. J. Lough, I. Manners, *Chem. Commun.* **2001**, 962–963; b) C. A. Jaska, K. Temple, A. J. Lough, I. Manners, *J. Am. Chem. Soc.* **2003**, *125*, 9424–9434; c) T. J. Clark, C. A. Russell, I. Manners, *J. Am. Chem. Soc.* **2006**, *128*, 9582–9583.
[20] Y. Kawano, M. Uruichi, M. Shimoi, S. Taki, T. Kawaguchi, T. Kakizawa, H. Ogino, *J. Am. Chem. Soc.* **2009**, *131*, 14946–14957.
[21] R. J. Keaton, J. M. Blacquiere, R. T. Baker, *J. Am. Chem. Soc.* **2007**, *129*, 1844–1845.
[22] a) A. Staubitz, A. P. M. Robertson, M. E. Sloan, I. Manners, *Chem. Rev.* **2010**, *110*, 4023–4078; b) A. Staubitz, A. P. M. Robertson, I. Manners, *Chem. Rev.* **2010**, *110*, 4079–4124.
[23] a) G. Alcaraz, S. Sabo-Etienne, *Angew. Chem.* **2010**, *122*, 7326; *Angew. Chem. Int. Ed.* **2010**, *49*, 7170–7179; b) C. W. Hamilton, R. T. Baker, A. Staubitz, I. Manners, *Chem. Soc. Rev.* **2009**, *38*, 279–293; c) T. M. Douglas, A. B. Chaplin, A. S. Weller, X. Yang, M. B. Hall, *J. Am. Chem. Soc.* **2009**, *131*, 15440–15456; d) A. Friedrich, M. Drees, S. Schneider, *Chem. Eur. J.* **2009**, *15*, 10339–10342; e) V. Pons, R. T. Baker, N. K. Szymczak, D. J. Heldebrant, J. C. Linehan, M. H. Matus, D. J. Grant, D. A. Dixon, *Chem. Commun.* **2008**, 6597–6599.
[24] a) X. Z. Yang, M. B. Hall, *J. Am. Chem. Soc.* **2008**, *130*, 1798–1799; b) X. Z. Yang, M. B. Hall, *J. Organomet. Chem.* **2009**, *694*, 2831–2838; c) Y. Luo, K. Ohno, *Organometallics* **2007**, *26*, 3597–3600; d) A. Paul, C. B. Musgrave, *Angew. Chem.* **2007**, *119*, 8301–8304; *Angew. Chem. Int. Ed.* **2007**, *46*, 8153–8156.
[25] M. Käß, A. Friedrich, M. Drees, S. Schneider, *Angew. Chem.* **2009**, *121*, 922–924; *Angew. Chem. Int. Ed.* **2009**, *48*, 905–907.
[26] A. B. Chaplin, A. S. Weller, *Angew. Chem.* **2010**, *122*, 591–594; *Angew. Chem. Int. Ed.* **2010**, *49*, 581–584.
[27] G. Alcaraz, L. Vendier, E. Clot, S. Sabo-Etienne, *Angew. Chem.* **2010**, *122*, 930–932; *Angew. Chem. Int. Ed.* **2010**, *49*, 918–920.
[28] R. Dallanegra, A. B. Chaplin, A. S. Weller, *Angew. Chem.* **2009**, *121*, 7007–7010; *Angew. Chem. Int. Ed.* **2009**, *48*, 6875–6878.
[29] N. Merle, G. Koicok-Köhn, M. F. Mahon, C. G. Frost, G. D. Ruggerio, A. S. Weller, M. C. Willis, *Dalton Trans.* **2004**, 3883–3892.
[30] C. J. Stevens, R. Dallanegra, A. B. Chaplin, A. S. Weller, S. A. Macgregor, B. Ward, D. McKay, G. Alcaraz, S. Sabo-Etienne, *Chem. Eur. J.* **2011**, *17*, 3011–3020.
[31] R. Dallanegra, A. B. Chaplin, J. Tsin, A. S. Weller, *Chem. Commun.* **2010**, *46*, 3092–3094. Crystallographic data are given for [Rh{P(iPr)$_2$(η^2-C_5H_7)}**B**]$^+$.
[32] a) A. D. Becke, *J. Chem. Phys.* **1993**, *98*, 5648–5652; b) J. P. Perdew, Y. Wang, *Phys. Rev. B* **1992**, *45*, 13244–13249.
[33] Gaussian 03, Revision C.02, M. J. Frisch, G. W. Trucks, H. B. Schlegel, G. E. Scuseria, M. A. Robb, J. R. Cheeseman, J. A. Montgomery, Jr., T. Vreven, K. N. Kudin, J. C. Burant, J. M. Millam, S. S. Iyengar, J. Tomasi, V. Barone, B. Mennucci, M. Cossi, G. Scalmani, N. Rega, G. A. Petersson, H. Nakatsuji, M. Hada, M. Ehara, K. Toyota, R. Fukuda, J. Hasegawa, M. Ishida, T. Nakajima, Y. Honda, O. Kitao, H. Nakai, M. Klene, X. Li, J. E. Knox, H. P. Hratchian, J. B. Cross, V. Bakken, C. Adamo, J. Jaramillo, R. Gomperts, R. E. Stratmann, O. Yazyev, A. J. Austin, R. Cammi, C. Pomelli, J. W. Ochterski, P. Y. Ayala, K. Morokuma, G. A. Voth, P. Salvador, J. J. Dannenberg, V. G. Zakrzewski, S. Dapprich, A. D. Daniels, M. C. Strain, O. Farkas, D. K. Malick, A. D. Rabuck, K. Raghavachari, J. B. Foresman, J. V. Ortiz, Q. Cui, A. G. Baboul, S. Clifford, J. Cioslowski, B. B. Stefanov, G. Liu, A. Liashenko, P. Piskorz, I. Komaromi, R. L. Martin, D. J. Fox, T. Keith, M. A. Al-Laham, C. Y. Peng, A. Nanayakkara, M. Challacombe, P. M. W. Gill, B. Johnson, W. Chen, M. W. Wong, C. Gonzalez, J. A. Pople, Gaussian, Inc., Wallingford CT, **2004**.
[34] D. Andrae, U. Häußermann, M. Dolg, H. Stoll, H. Preuß, *Theor. Chim. Acta* **1990**, *77*, 123–141.
[35] a) K. Fukui, *J. Phys. Chem.* **1970**, *74*, 4161–4163; b) C. Gonzalez, H. B. Schlegel, *J. Chem. Phys.* **1989**, *90*, 2154–2161.
[36] a) M. T. Cancès, B. Mennucci, J. Tomasi, *J. Chem. Phys.* **1997**, *107*, 3032–3041; b) M. Cossi, V. Barone, B. Mennucci, J. Tomasi, *Chem. Phys. Lett.* **1998**, *286*, 253–260; c) B. Mennucci, J. Tomasi, *J. Chem. Phys.* **1997**, *106*, 5151–5158.

Received: July 29, 2011
Published online: November 22, 2011

